JB
Journals.ASM.org

Critical Components of the Conjugation Machinery of the Integrative and Conjugative Element ICE*Bs1* of *Bacillus subtilis*

Cori T. Leonetti,[a] Matt A. Hamada,[a] Stephanie J. Laurer,[a] Matthew P. Broulidakis,[a] Kyle J. Swerdlow,[a] Catherine A. Lee,[b] Alan D. Grossman,[b] Melanie B. Berkmen[a]

Department of Chemistry and Biochemistry, Suffolk University, Boston, Massachusetts, USA[a]; Department of Biology, Massachusetts Institute of Technology, Cambridge, Massachusetts, USA[b]

ABSTRACT

Conjugation, or mating, plays a profound role in bacterial evolution by spreading genes that allow bacteria to adapt to and colonize new niches. ICE*Bs1*, an integrative and conjugative element of *Bacillus subtilis*, can transfer itself and mobilize resident plasmids. DNA transfer is mediated by a type IV secretion system (T4SS). Characterized components of the ICE*Bs1* T4SS include the conserved VirB4-like ATPase ConE, the bifunctional cell wall hydrolase CwlT, and the presumed VirD4-like coupling protein ConQ. A fusion of ConE to green fluorescent protein (GFP) localizes to the membrane preferentially at the cell poles. One or more ICE*Bs1* proteins are required for ConE's localization at the membrane, as ConE lacks predicted transmembrane segments and ConE-GFP is found dispersed throughout the cytoplasm in cells lacking ICE*Bs1*. Here, we analyzed five ICE*Bs1* genes to determine if they are required for DNA transfer and/or ConE-GFP localization. We found that *conB*, *conC*, *conD*, and *conG*, but not *yddF*, are required for both ICE*Bs1* transfer and plasmid mobilization. All four required genes encode predicted integral membrane proteins. *conB* and, to some extent, *conD* were required for localization of ConE-GFP to the membrane. Using an adenylate cyclase-based bacterial two-hybrid system, we found that ConE interacts with ConB. We propose a model in which the ICE*Bs1* conjugation machinery is composed of ConB, ConC, ConD, ConE, ConG, CwlT, ConQ, and possibly other ICE*Bs1* proteins, and that ConB interacts with ConE, helping to recruit and/or maintain ConE at the membrane.

IMPORTANCE

Conjugation is a major form of horizontal gene transfer and has played a profound role in bacterial evolution by moving genes, including those involved in antibiotic resistance, metabolism, symbiosis, and infectious disease. During conjugation, DNA is transferred from cell to cell through the conjugation machinery, a type of secretion system. Relatively little is known about the conjugation machinery of Gram-positive bacteria. Here, we analyzed five genes of the integrative and conjugative element ICE*Bs1* of *Bacillus subtilis*. Our research identifies four new components of the ICE*Bs1* conjugation machinery (ConB, ConC, ConD, and ConG) and shows an interaction between ConB and ConE that is required for ConE to associate with the cell membrane.

Conjugation is a major form of horizontal gene transfer and plays a profound role in bacterial evolution and the acquisition of new traits (1–3). Conjugation can spread antibiotic resistance and disseminate genes involved in symbiosis, degradation of pollutants, metabolism, and pathogenesis. Conjugative elements encode specialized DNA translocation channels classified as type IV secretion systems (T4SSs) (4–7). T4SSs are composed of many interacting proteins that span the envelope of the donor cell. In addition to transferring the conjugative DNA element, the conjugation machinery also can mobilize resident plasmids or other DNA elements that do not encode their own machinery.

There is a rich body of mechanistic and structural information on the T4SSs of Gram-negative bacteria (4, 7, 8). The Gram-negative T4SS generally is composed of 11 conserved mating-pair formation proteins (VirB1-VirB11, using the nomenclature of the *Agrobacterium tumefaciens* pTi plasmid) that form the DNA translocation channel along with a so-called coupling protein ATPase (VirD4) that delivers the relaxase-conjugative DNA nucleoprotein complex to the channel.

In contrast, much less is known about the minimized T4SSs of Gram-positive bacteria, which seem to be composed of a subset of the Gram-negative T4SS components (6–8). Conjugative elements from Gram-positive organisms generally encode homologs to three T4SS proteins from Gram-negative bacteria: a VirD4-like coupling protein, a VirB1-like cell wall hydrolase, and a VirB4-like ATPase. In addition, elements from Gram-positive bacteria encode proteins with similar structures and/or predicted membrane topologies and sizes to VirB3, VirB6, and VirB8. Many Gram-positive elements encode additional proteins that also might form part of the machinery.

The T4SSs of Gram-positive bacteria feature several significant differences from those found in Gram-negative bacteria, which is not surprising given the differences in the cell envelopes and se-

Received 27 February 2015 **Accepted** 14 May 2015
Accepted manuscript posted online 26 May 2015
Citation Leonetti CT, Hamada MA, Laurer SJ, Broulidakis MP, Swerdlow KJ, Lee CA, Grossman AD, Berkmen MB. 2015. Critical components of the conjugation machinery of the integrative and conjugative element ICE*Bs1* of *Bacillus subtilis*. J Bacteriol 197:2558–2567. doi:10.1128/JB.00142-15.
Editor: P. J. Christie
Address correspondence to Melanie B. Berkmen, mberkmen@suffolk.edu.
C.T.L., M.A.H., and S.J.L. are co-first authors.
Copyright © 2015, American Society for Microbiology. All Rights Reserved.
doi:10.1128/JB.00142-15

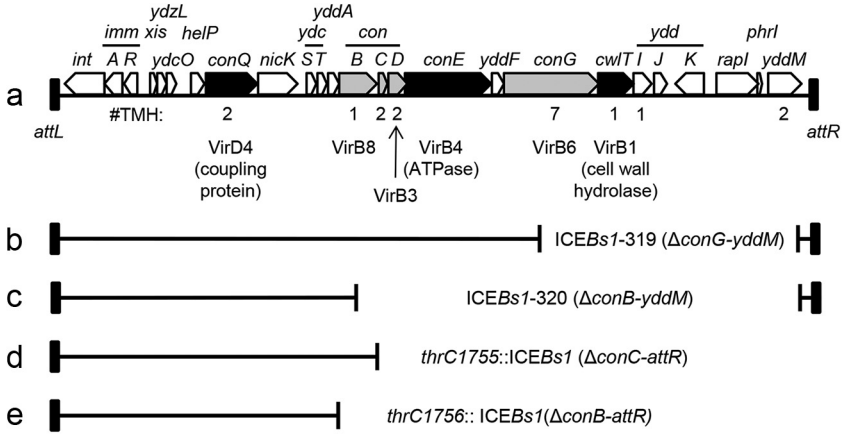

FIG 1 Genetic structure of ICE*Bs1* and its derivatives. (a) Schematic of ICE*Bs1* integrated at the normal attachment site, *attB*. Each ORF (arrowed box oriented in the direction of its transcription) and *attL* and *attR* (black boxes) are indicated. Previously characterized genes that encode ICE*Bs1* conjugation machinery are shaded in black. Genes shown here to be required for conjugation are shaded in gray. The number of predicted transmembrane helices (TMH) for each protein is indicated below each gene. Predictions were obtained from Polyphobius, an HMM topology prediction program that uses homology information (59), guided by the bacterial subcellular location and secretion prediction program LocateP (60). Other topology programs yield similar but not identical predictions. Genes that encode proteins with homology or predicted structural similarity or membrane topology to *A. tumefaciens* pTi VirB/D T4SS components are designated below. An antibiotic resistance marker (*kan* or *cam*) is inserted in *rapI-phrI* in most strains but is not shown. (b to e) Diagram of truncated ICE*Bs1* derivatives that were used to analyze ConE-GFP localization. (b and c) Derivatives of ICE*Bs1*, ICE*Bs1*-319 (Δ*conG-yddM*) and ICE*Bs1*-320 (Δ*conB-yddM*), at *attB* have the genes indicated by the horizontal line from *attL* to the middle of *conG* (b) or *conB* (c). (d and e) Truncated ICE*Bs1* derivatives integrated at *thrC*, *thrC1755*::ICE*Bs1* (Δ*conC-attR*), and *thrC*, *thrC1756*::ICE*Bs1* (Δ*conB-attR*), have the genes indicated by the horizontal line from *attL* and up to and including *conB* (D) or *yddA* (e).

quences of the component proteins (6, 7). For example, Gram-positive elements do not encode homologs of any components that comprise the Gram-negative outer membrane core complex, which plays crucial roles in T4SS assembly and gating. In addition, conjugative cell wall hydrolases are critical for conjugation in Gram-positive organisms (9–12), whereas they generally are dispensable for most Gram-negative ones (13–15).

ICE*Bs1* is an integrative and conjugative element (ICE) found in the chromosome of *Bacillus subtilis* (reviewed in reference 16). The genes needed for transfer of ICE*Bs1* are related to those from Tn*916* and ICE*St1* and other conjugative elements. ICE*Bs1* contains approximately two dozen open reading frames (ORFs), many of which have been characterized previously for their roles in regulation, DNA processing, DNA replication, and conjugation (Fig. 1a) (9, 17–28). ICE*Bs1* normally resides stably integrated in *trnS-leu2*, the gene for a leucine tRNA, unless its major operon is derepressed (20). Derepression and subsequent excision and mating are induced upon DNA damage or when cells are crowded by potential recipients that do not have ICE*Bs1*. Upon induction, ICE*Bs1* can transfer itself and mobilize resident plasmids, such as pBS42, that lack dedicated mobilization functions (26). Although plasmid mobilization requires ICE*Bs1*'s putative coupling protein ConQ, it does not require the ICE*Bs1* conjugative relaxase, ICE*Bs1* excision, or cotransfer with ICE*Bs1*. Thus, ICE*Bs1* is required to build the conjugation machinery allowing for mobilization to occur.

By analogy to other conjugation systems, the ICE*Bs1* conjugation machinery likely is composed of several interacting proteins. So far, the putative coupling protein ConQ (26), a VirB1-like cell wall hydrolase, CwlT (9), and a VirB4-like ATPase, ConE (27), are characterized components (Fig. 1a). Previously, we found that a fusion of ConE to a monomeric green fluorescent protein (GFP) localizes to the periphery of the cell membrane, with a large concentration found at the cell poles (27). One or more ICE*Bs1* proteins appear to be required for ConE to associate with the membrane, as ConE lacks predicted transmembrane segments and is found dispersed throughout the cytoplasm in cells lacking ICE*Bs1*.

We were interested in identifying other ICE*Bs1* genes needed for conjugation and determining which ICE*Bs1* proteins were needed for ConE to localize to the membrane. We constructed deletions in five ICE*Bs1* genes: *conB*, *conC*, *conD*, *conG* (previously *yddB*, *yddC*, *yddD*, and *yddG*, respectively), and *yddF* (Fig. 1a). We then characterized the effects of the deletions on ICE*Bs1* transfer, plasmid mobilization, and localization of ConE-GFP. Together, our results are consistent with a model in which the ICE*Bs1* conjugation machinery is composed of putative transmembrane proteins ConB, ConC, ConD, and ConG, along with the previously described ATPase ConE, cell wall hydrolase CwlT, and coupling protein ConQ. Furthermore, our results indicate that the peripheral membrane protein ConE is recruited to or kept at the membrane at least in part through direct interaction with ConB.

MATERIALS AND METHODS

Media and growth conditions. For *B. subtilis* and *Escherichia coli* strains, routine growth and strain constructions were done in LB medium. For all reported experiments with *B. subtilis*, cells were grown first in liquid LB at 37°C to an optical density at 600 nm (OD_{600}) of ~1.0. Cells then were diluted ~50-fold into LB or S7 defined minimal medium (29) with morpholinepropanesulfonic acid (MOPS) buffer at 50 mM rather than 100 mM, containing 1% glucose and 0.1% glutamate and supplemented with auxotrophic requirements (40 μg/ml tryptophan, 40 μg/ml phenylalanine, 200 μg/ml threonine) as needed. Antibiotics were used at standard concentrations (30). For induction of ICE*Bs1*, 1 mM IPTG (isopropyl-β-D-thiogalactopyranoside) was added for 1 to 2 h to overexpress *rapI* from Pspank(hy) in single copy on the chromosome at *amyE*, i.e., *amyE*::[(Pspank(hy)-*rapI*) *spc*], as described previously (20).

Strains, alleles, and plasmids. *E. coli* strains used for routine cloning were NEB 5α (New England BioLabs), AG115 (MC1061 F′ *lacI*^{q} *lacZ*::Tn*5*), and AG1111 (MC1061 F′ *lacI*^{q} *lacZ*M15 Tn*10*). *B. subtilis* strains

TABLE 1 *B. subtilis* strains used[a]

Strain	Relevant genotype and/or characteristic(s) (reference)
CAL89	ICE*Bs1*^{0} *comK*::*spc str-84* (20)
CAL419	ICE*Bs1*^{0} *comK*::*cat str-84* (25)
JMA168	Δ(*rapI phrI*)*342*::*kan amyE*::[(Pspank(hy)-*rapI*) *spc*] (20)
MMB968	Δ(*rapI phrI*)*342*::*kan amyE*::[(Pspank(hy)-*rapI*) *spc*] *lacA*::[Pxis-(*conD conE-mgfpmut2*) *tet*] (27)
MMB1247	Δ(*rapI phrI*)*342*::*kan* [Δ*conQ848* (unmarked)] *amyE*::[(Pspank(hy)-*rapI*) *spc*] *lacA*::[Pxis-(*conD conE-mgfpmut2*) *tet*]
MMB1271	Δ(*rapI phrI*)*342*::*kan* [*conC*Δ(5-81) (unmarked)] *amyE*::[(Pspank(hy)-*rapI*) *spc*]
MMB1273	Δ(*rapI phrI*)*342*::*kan* [*yddF*Δ(5-103) (unmarked)] *amyE*::[(Pspank(hy)-*rapI*) *spc*]
MMB1274	Δ(*rapI phrI*)*342*::*kan* [*conD*Δ(5-131) (unmarked)] *amyE*::[(Pspank(hy)-*rapI*) *spc*]
MMB1275	Δ(*rapI phrI*)*342*::*kan* [*conB*Δ(9-350) (unmarked)] *amyE*::[(Pspank(hy)-*rapI*) *spc*]
MMB1283	Δ(*rapI phrI*)*342*::*kan* [*conG*Δ(5-805) (unmarked)] *amyE*::[(Pspank(hy)-*rapI*) *spc*]
MMB1293	Δ(*rapI phrI*)*342*::*kan* [*conC*Δ(5-81) (unmarked)] *amyE*::[(Pspank(hy)-*rapI*) *spc*] *lacA*::[Pxis-(*conD conE-mgfpmut2*) *tet*]
MMB1297	Δ(*rapI phrI*)*342*::*kan* [*conB*Δ(9-350) (unmarked)] *amyE*::[(Pspank(hy)-*rapI*) *spc*] *lacA*::[Pxis-(*conD conE-mgfpmut2*) *tet*]
MMB1299	Δ(*rapI phrI*)*342*::*kan* [*conG*Δ(5-805) (unmarked)] *amyE*::[(Pspank(hy)-*rapI*) *spc*] *lacA*::[Pxis-(*conD conE-mgfpmut2*) *tet*]
MMB1343	Δ(*rapI phrI*)*342*::*kan* [*yddF*Δ(5-103) (unmarked)] *amyE*::[(Pspank(hy)-*rapI*) *spc*] *lacA*::[Pxis-(*conD conE-mgfpmut2*) *tet*]
MMB1390	Δ(*rapI phrI*)*342*::*kan* [*conC*Δ(5-81) (unmarked)] *amyE*::[(Pspank(hy)-*rapI*) *spc*] *thrC*::[(Pspank(hy)-*conC*) *mls*]
MMB1393	Δ(*rapI phrI*)*342*::*kan* [*conG*Δ(5-805) (unmarked)] *amyE*::[(Pspank(hy)-*rapI*) *spc*] *thrC*::[(Pspank(hy)-*conG*) *mls*]
MMB1397	Δ(*rapI phrI*)*342*::*kan* [*conD*Δ(5-131) (unmarked)] *amyE*::[(Pspank(hy)-*rapI*) *spc*] *thrC*::[(Pspank(hy)-*conD*) *mls*]
MMB1412	Δ(*rapI phrI*)*342*::*kan* [*conB*Δ(9-350) (unmarked)] *amyE*::[(Pspank(hy)-*rapI*) *spc*] *thrC325*::[(ICE*Bs1*-311 (Δ*attR*100::*tet*)) *mls*]
MMB1413	Δ(*rapI phrI*)*342*::*kan* [*conC*Δ(5-81) (unmarked)] *amyE*::[(Pspank(hy)-*rapI*) *spc*] *thrC325*::[(ICE*Bs1*-311 (Δ*attR*100::*tet*)) *mls*]
MMB1419	Δ(*rapI phrI*)*342*::*kan* [*conG*Δ(5-805) (unmarked)] *amyE*::[(Pspank(hy)-*rapI*) *spc*] *thrC325*::[(ICE*Bs1*-311 (Δ*attR*100::*tet*)) *mls*]
MMB1425	ICE*Bs1*-319::*kan amyE*::[(Pspank(hy)-*rapI*) *spc*] *lacA*::[Pxis-(*conD conE-mgfpmut2*) *tet*]
MMB1426	ICE*Bs1*-320::*kan amyE*::[(Pspank(hy)-*rapI*) *spc*] *lacA*::[Pxis-(*conD conE-mgfpmut2*) *tet*]
MMB1429	Δ(*rapI phrI*)*342*::*kan* [*conD*Δ(5-131) (unmarked)] *amyE*::[(Pspank(hy)-*rapI*) *spc*] *thrC325*::[(ICE*Bs1*-311 (Δ*attR100*::*tet*)) *mls*]
MMB1473	Δ(*rapI phrI*)*342*::*kan amyE*::[(Pspank(hy)-*rapI*) *spc*]; pBS42 (*cat*)
MMB1474	Δ(*rapI phrI*)*342*::*kan* [*conB*Δ(9-350) (unmarked)] *amyE*::[(Pspank(hy)-*rapI*) *spc*]; pBS42 (*cat*)
MMB1476	Δ(*rapI phrI*)*342*::*kan* [*conC*Δ(5-81) (unmarked)] *amyE*::[(Pspank(hy)-*rapI*) *spc*]; pBS42 (*cat*)
MMB1477	Δ(*rapI phrI*)*342*::*kan* [*conC*Δ(5-81) (unmarked)] *amyE*::[(Pspank(hy)-*rapI*) *spc*] *thrC*::[(Pspank(hy)-*conC*) *mls*]; pBS42 (*cat*)
MMB1478	Δ(*rapI phrI*)*342*::*kan* [*conD*Δ(5-131) (unmarked)] *amyE*::[(Pspank(hy)-*rapI*) *spc*]; pBS42 (*cat*)
MMB1479	Δ(*rapI phrI*)*342*::*kan* [*conD*Δ(5-131) (unmarked)] *amyE*::[(Pspank(hy)-*rapI*) *spc*] *thrC*::[(Pspank(hy)-*conD*) *mls*]; pBS42 (*cat*)
MMB1480	Δ(*rapI phrI*)*342*::*kan* [*conE*(*K476E*) (unmarked)] *amyE*::[(Pspank(hy)-*rapI*) *spc*]; pBS42 (*cat*)
MMB1481	Δ(*rapI phrI*)*342*::*kan* [*conE*(*K476E*) (unmarked)] *amyE*::[(Pspank(hy)-*rapI*) *spc*] *thrC*::[(Pxis-(*conD conE-lacZ*)) *mls*]; pBS42 (*cat*)
MMB1482	Δ(*rapI phrI*)*342*::*kan* [*yddF*Δ(5-103) (unmarked)] *amyE*::[(Pspank(hy)-*rapI*) *spc*]; pBS42 (*cat*)
MMB1483	Δ(*rapI phrI*)*342*::*kan* [*yddF*Δ(5-103) (unmarked)] *amyE*::[(Pspank(hy)-*rapI*) *spc*] *thrC*::[(Pspank(hy)-*yddF*) *mls*]; pBS42 (*cat*)
MMB1484	Δ(*rapI phrI*)*342*::*kan* [*conG*Δ(5-805) (unmarked)] *amyE*::[(Pspank(hy)-*rapI*) *spc*]; pBS42 (*cat*)
MMB1485	Δ(*rapI phrI*)*342*::*kan* [*conG*Δ(5-805) (unmarked)] *amyE*::[(Pspank(hy)-*rapI*) *spc*] *thrC*::[(Pspank(hy)-*conG*) *mls*]; pBS42 (*cat*)
MMB1547	Δ(*rapI phrI*)::*cat amyE*::[(Pspank(hy)-*rapI*) *spc*] *conE*::pMMB1530 (*conE-mgfpmut2 kan*)
MMB1548	Δ(*rapI phrI*)::*cat* [*conC*Δ(5-81) (unmarked)] *amyE*::[(Pspank(hy)-*rapI*) *spc*] *conE*::pMMB1530 (*conE-mgfpmut2 kan*)
MMB1549	Δ(*rapI phrI*)::*cat* [*conD*Δ(5-131) (unmarked)] *amyE*::[(Pspank(hy)-*rapI*) *spc*] *conE*::pMMB1530 (*conE-mgfpmut2 kan*)
MMB1550	Δ(*rapI phrI*)::*cat* [*conB*Δ(9-350) (unmarked)] *amyE*::[(Pspank(hy)-*rapI*) *spc*] *conE*::pMMB1530 (*conE-mgfpmut2 kan*)
MMB1715	ICE*Bs1*^{0} *thrC*::[(Pspank(hy)-(*conB conC conD conE-mgfpmut2*)) *mls*]
MMB1735	Δ(*rapI phrI*)*342*::*kan* [*conB*Δ(9-350) (unmarked)] *amyE*::[(Pspank(hy)-*rapI*) *spc*] *thrC*::[(Pspank(hy)-*conB*) *mls*]
MMB1760	Δ(*rapI phrI*)*342*::*kan* [*conB*Δ(9-350) (unmarked)] *amyE*::[(Pspank(hy)-*rapI*) *spc*] *thrC*::[(Pspank(hy)-*conB*) *mls*]; pBS42 (*cat*)
MMB1763	Δ(*rapI phrI*)*342*::*kan* [*conB*Δ(9-350) (unmarked)] *amyE*::[(Pspank(hy)-*rapI*) *spc*] *lacA*:: [Pxis-(*conD conE-mgfpmut2*) *tet*] *thrC1755*::[ICE*Bs1* (Δ*conC-attR*::*cat*) *mls*]
MMB1764	Δ(*rapI phrI*)*342*::*kan* [*conB*Δ(9-350) (unmarked)] *amyE*::[(Pspank(hy)-*rapI*) *spc*] *lacA*::[Pxis-(*conD conE-mgfpmut2*) *tet*] *thrC1756*::[ICE*Bs1* (Δ*conB-attR*::*cat*) *mls*]

[a] All strains are derived from JH642 (31) and contain *pheA1* and *trpC2*.

and relevant genotypes are listed in Table 1; all are derivatives of JH642 containing the *trpC2* and *pheA1* mutations (31). *B. subtilis* strains were constructed by natural transformation (30). Strains cured of ICE*Bs1* (ICE*Bs1*^{0}), the spontaneous streptomycin resistance allele (*str-84*), the *amyE*::[Pspank(hy)-*rapI spc*] allele, and Δ(*rapI phrI*)*342*::*kan* were described previously (20). The unmarked *conE*(*K476E*) allele (with the K-to-E change at position 476 encoded by *conE*), the complementation construct *thrC*::[(Pxis-(*conD conE-lacZ*)) *mls*], and the *lacA*::[P*xis*-(*conD conE-mgfpmut2*) *tet*] allele expressing *conD* and *conE-gfp* from the ectopic locus *lacA* were described previously (27). The *conQ848* deletion was described previously (26). The *thrC325*::[(ICE*Bs1*-311 (Δ*attR*::*tet*)) *mls*] allele, containing ICE*Bs1* inserted at *thrC*, is incapable of excision due to deletion of the right attachment site *attR* as described previously (25). The truncation alleles ICE*Bs1*-319 (Fig. 1b) and ICE*Bs1*-320 (Fig. 1c) at *attB* have been described previously (25). pBS42 uses rolling-circle replication, expresses chloramphenicol resistance in *B. subtilis*, lacks *mob-oriT*, and can be mobilized by ICE*Bs1* (26). All inserts in newly cloned plasmids were verified by sequencing.

Construction of unmarked in-frame gene deletions. The basic strategy for constructing unmarked gene deletions was similar to that previously described for construction of *nicK306* (25). All gene deletions are unmarked and in frame, and they keep the upstream and downstream genes intact. *conB*Δ(9-350) deletes codons 9 through 350 of *conB*, resulting in the fusion of codons 1 through 8 to codons 351 through 357. *conC*Δ(5-81) deletes codons 5 through 81 of *conC*, resulting in the fusion of codons 1 through 4 to the last codon, 82. *conD*Δ(5-131) deletes codons 5 through 131 of *conD*, resulting in the fusion of codons 1 through 4 to codons 132 through 174. *yddF*Δ(5-103) deletes codons 5 through 103 of

yddF, resulting in the fusion of codons 1 through 4 to codons 104 through 108. *conG*Δ(5-805) deletes codons 5 through 805 of *conG*, resulting in the fusion of codons 1 through 4 to codons 806 through 815. The splice-overlap extension (SOE) PCR method (32) was used to generate DNA fragments containing the alleles. These fragments were cloned into the chloramphenicol resistance vector pEX44 (33) upstream of *lacZ*. The resulting plasmids were pMMB1257 for *conB*Δ(9-350), pMMB1251 for *conC*Δ(5-81), pMMB1253 for *conD*Δ(5-131), pMMB1252 for *yddF*Δ(5-103), and pMMB1254 for *conG*Δ(5-805). To replace the wild-type (wt) allele with the deleted gene, each plasmid first was integrated onto the chromosome of strain JMA168 by single crossover. The resulting strain was grown without selection for at least 20 generations, and loss of the plasmid was screened for by loss of both *lacZ* and chloramphenicol resistance. Detection of the desired unmarked deletion was confirmed by PCR.

Construction of ICE*Bs1* single-gene complementation alleles. Complemented genes were cloned downstream of the IPTG-inducible promoter Pspank(hy). The *thrC*::[(Pspank(hy)-*conC*) *mls*] allele was constructed to express *conC*. *conC* was cloned into pCAL838, downstream of Pspank(hy), creating plasmid pMMB1338. pCAL838 allows for double crossover at the *thrC* locus in *B. subtilis* and contains Pspank(hy), *lacI*, and *mls*. pMMB1338 was transformed into *B. subtilis* to create the *thrC*::[(Pspank(hy)-*conC*) *mls*] allele. A similar strategy was used to produce *thrC*::[(Pspank(hy)-*conB*) *mls*] from plasmid pMMB1695, *thrC*::[(Pspank(hy)-*conD*) *mls*] from plasmid pMMB1339, *thrC*::[(Pspank(hy)-*yddF*) *mls*] from plasmid pMMB1340, and *thrC*::[(Pspank(hy)-*conG*) *mls*] from plasmid pMMB1341. For pMMB1695, an ATG start codon was used to replace the TTG native *conB* start codon, improving complementation (data not shown). For several genes tested, complementation was similar when genes were expressed from either Pspank(hy) or the ICE*Bs1* promoter Pxis but was inferior when expressed from Pspank (data not shown).

Construction of truncated ICE*Bs1* complementation alleles. Complementation of ConE-GFP localization in the Δ*conB* strain was tested using truncated ICE*Bs1* complementation constructs that cannot excise or transfer, similar to the strategy described previously (26). The truncated ICE*Bs1* derivative integrated at *thrC*, *thrC1755*::[ICE*Bs1* (Δ*conC-attR*::*cat*) *mls*], contains all of the ICE*Bs1* genes upstream of and including *conB* (Fig. 1d). The construct *thrC1756*::[ICE*Bs1* (Δ*conB-attR*::*cat*) *mls*] is essentially the same ICE*Bs1* insertion at *thrC*, but it is missing *conB* (Fig. 1e). These alleles were constructed by transforming CAL1496, harboring *thrC325*::[(ICE*Bs1*-311 (Δ*attR*::*tet*)) *mls*], with SOE PCR products that deleted the desired downstream region of ICE*Bs1*, replacing the tetracycline resistance gene with a chloramphenicol resistance gene.

Conversion of Δ(*rapI phrI*)*342*::*kan* to Δ(*rapI phrI*)::*cat*. The Δ(*rapI phrI*)*342*::*kan* allele (20) was altered to confer chloramphenicol resistance, creating the Δ(*rapI phrI*)::*cat* allele. JMA168 was transformed with linearized pMMB1487, selecting for resistance to chloramphenicol and screening for kanamycin sensitivity. pMMB1487 was constructed through isothermal assembly (34) so that it contains the *cat* gene flanked by *yddK-rapI* and *yddM-yddN*.

Construction of *conE-gfp* expressed from the *conE* locus in ICE*Bs1*. Strains MMB1547 to MMB1550 have the *conE* gene fused in frame to monomeric *gfpmut2* (*mgfpmut2*) at its native locus in ICE*Bs1*. These strains were made by integrating pMMB1530 into the *B. subtilis* chromosome via a single crossover into *conE*. pMMB1530 contains the 3′ end of *conE* fused to DNA sequence encoding a 23-amino-acid linker and *mgfpmut2*. The plasmid was introduced into *B. subtilis* by transformation and selection for kanamycin resistance. pMMB1530 was constructed by ligating the XhoI- and SphI-cut vector from pMMB1445 with the XhoI- and SphI-cut fragment encoding the 23-amino-acid linker and *mgfpmut2* from pLS31 (35). pMMB1445 was constructed by inserting a PCR fragment containing the 3′ end of *conE* into pKL168 (36) digested with EcoRI and XhoI.

Construction of Pspank(hy) *conB conC conD conE-gfp* at *thrC*. pMMB1702 was transformed into *B. subtilis* to create the *thrC*::[(Pspank(hy)-(*conB conC conD conE-mgfpmut2*) *mls*] allele that expresses *conB*, *conC*, *conD*, and *conE-mgfpmut2*. pMMB1702 was constructed via isothermal assembly (34) of the PCR inserts *conB conC conD* and *conE-mgfpmut2* into pCAL838 downstream of Pspank(hy). An ATG start codon was used to replace the native *conB* start codon, TTG.

Construction of bacterial two-hybrid protein fusion plasmids. ICE*Bs1* genes were cloned in frame into vectors carrying either the N-terminal (T25) or C-terminal (T18) portion of the *Bordetella pertussis cyaA* gene for adenylate cyclase as previously described (37). The plasmids encoding N- and C-terminal fusions of T18 to ConE were constructed by cloning into the BamHI/PstI sites of the vectors. pMMB1457 and pMMB1458 encode ampicillin resistance along with ConE-T18 and T18-ConE, respectively. Plasmids encoding N- and C-terminal fusions of T25 to ConB or ConD were constructed via isothermal assembly (34). pMMB1603, pMMB1604, pMMB1605, and pMMB1626 encode kanamycin resistance along with T25-ConD, ConB-T25, ConD-T25, and T25-ConB, respectively.

Bacterial two-hybrid interaction assays. The bacterial two-hybrid assays were performed with methods similar to those in a prior report (37). Two plasmids (one containing a T18 fusion and another containing a T25 fusion) were cotransformed into *E. coli* BTH101 [F^- *cya-99 araD139 gal15 galK16 rpsL1* (Str^r) *hsdR2 mcrA1 mcrB1*] competent cells. For negative controls, an empty vector was cotransformed with a T18/25 fusion protein or another empty vector. For qualitative analysis, the transformations were plated on MacConkey base agar supplemented with 0.1% maltose, 0.1 mg/ml ampicillin, 0.05 mg/ml kanamycin, and 0.5 mM isopropyl β-D-1-thiogalactopyranoside (IPTG). The plates were incubated at 37°C overnight and then at room temperature (~20°C) for an additional 24 h for visual inspection of colony color. For quantitative assays, cells were grown with shaking in LB containing 0.1 mg/ml ampicillin, 0.05 mg/ml kanamycin, and 0.5 mM IPTG at 30°C overnight for 14 to 16 h. β-Galactosidase activity was quantified as previously described (38). The reported results are averages from at least four independent experiments.

Mating assays. ICE*Bs1* mating was assayed as described previously (20). Briefly, donor cells contained a kanamycin resistance gene in ICE*Bs1*. Recipient cells (strain CAL419) lacked ICE*Bs1* (ICE*Bs1*^{0}) and were distinguishable from donors by being streptomycin resistant (*str-84*). Recipients were *comK* null to prevent acquisition of DNA via transformation. Cells were grown for at least four generations to mid-exponential phase (OD_{600} of ~0.35) in minimal medium. ICE*Bs1* was induced in donors by addition of IPTG (1 mM) to induce expression of *rapI* from Pspank(hy). Donors and recipients were mixed 1:1 and filtered onto sterile cellulose nitrate membrane filters (0.2 μm pore size). Filters were placed in petri dishes containing Spizizen's minimal salts (30) with 1.5% agar and incubated at 37°C for 3 h. Cells were washed off the filter, and the number of transconjugants was measured by determining the number of kanamycin- and streptomycin-resistant CFU after the mating. The number of donors was measured by determining the number of kanamycin-resistant CFU after the mating. Percent mating is the number of transconjugant CFU per donor CFU times 100. The reported results are averages from at least three independent experiments.

Plasmid mobilization assays. Mobilization of plasmid pBS42 by ICE*Bs1* was assayed essentially as described previously (26), similar to the mating assay described above. In addition to containing ICE*Bs1*, donor cells contained the plasmid pBS42 and were grown with chloramphenicol (2.5 μg/ml) and kanamycin (2.5 μg/ml) to maintain selection of the plasmid and ICE*Bs1*, respectively. The recipient strain (CAL89) was ICE*Bs1*^{0}, streptomycin resistant (*str-84*), and *comK* null. Cells were grown for at least four generations to mid-exponential phase in LB medium before ICE*Bs1* was induced in donors by addition of IPTG (1 mM) to induce expression of *rapI* from Pspank(hy). Mating was performed on filters as described above. The number of pBS42 transconjugants was measured by determining the number of chloramphenicol- and streptomycin-resistant CFU. The number of donors was measured by determining the number of chloramphenicol-resistant CFU after the mating. Plasmid mobilization efficiencies were calculated as the number of transconjugant CFU per

donor CFU times 100. Transconjugants receiving ICE*Bs1* also were monitored as described above for mating assays. The reported results are averages from at least three independent experiments.

Live-cell fluorescence microscopy. Microscopy was performed as described previously (39). Cells were grown for at least four generations to mid-exponential phase in minimal medium. ICE*Bs1* was induced by addition of IPTG (1 mM) to induce expression of *rapI* from Pspank(hy). Experiments using ConE-GFP were done with strains that also contained a wild-type version of *conE* in ICE*Bs1*, except where noted. Live cells were immobilized on pads of 1% agarose containing Spizizen's minimal salts and visualized at room temperature. Some images were captured with a Nikon E800 microscope equipped with a 100× differential interference contrast objective, a Hamamatsu digital camera, and Chroma filter set 41012 (for GFP). Improvision Openlabs 4.0 software was used to process these images. The remaining images were captured with a Nikon H550L microscope equipped with a 100× Plan Fluor phase-contrast objective, a high-resolution monochrome cooled charge-coupled-device Andor digital camera, and Chroma filter set 96362 (for GFP). NIS Nikon Elements 4.0 software was used to process these images. Each strain was examined in at least three independent experiments.

RESULTS

***conB*, *conC*, *conD*, and *conG* (but not *yddF*) are required for the conjugative transfer of ICE*Bs1*.** We analyzed five ICE*Bs1* genes (*conB*, *conC*, *conD*, *yddF*, and *conG*) (Fig. 1a), as each had characteristics that suggested it encoded a component of the ICE*Bs1* T4SS. ConB is a putative bitopic membrane protein homologous to conjugation proteins that are structurally similar, but not phylogenetically related, to VirB8 (40, 41). ConC is a putative integral membrane protein with two predicted transmembrane helices (8). Although ConC homologs are not widespread, some conjugative elements in Gram-positive organisms encode proteins of similar size and predicted topology. ConD contains two transmembrane helices and resembles VirB3 in terms of size and predicted topology (7, 8). *yddF* encodes a putative DNA-binding protein that is found mainly in crenarchaeal viruses (42, 43). It was analyzed here given its proximity to other predicted ICE*Bs1* T4SS genes (Fig. 1a) and the modular nature of ICEs where genes of shared function are often linked (44, 45). Lastly, *conG* encodes a conserved putative polytopic membrane protein analogous to VirB6 and was previously shown to be involved in ICE*Bs1* conjugation (7).

We constructed in-frame unmarked deletions of *conB*, *conC*, *conD*, *yddF*, and *conG* in ICE*Bs1* to determine whether these genes were required for mating. We compared mating efficiencies of ICE*Bs1* from donor strains containing the various deletions into recipient *B. subtilis* cells lacking the conjugative element. The donor ICE*Bs1* contained a kanamycin resistance marker that had been inserted to allow selection and monitoring of ICE*Bs1* acquisition (20). We found that an ICE*Bs1*$^+$ donor strain transferred with an average mating frequency of ~3% (percent transconjugant CFU per donor CFU) (Fig. 2, row a), as seen previously (20). Conjugation was undetectable from Δ*conB*, Δ*conC*, Δ*conD*, or Δ*conG* donor strains (Fig. 2, rows b, d, f, and i). Given our limit of detection, we estimate that mating is down at least 300,000-fold for each. The Δ*yddF* donor strain mated in a fashion similar to that of wild-type *B. subtilis* cells (Fig. 2, row h).

The defect in mating caused by each gene deletion was complemented at least partially when the appropriate gene was reinserted at *thrC*, outside ICE*Bs1* (Fig. 2). Only the *conG* complementation construct restored mating to near wild-type efficiency (Fig. 2, row j). Mating was restored at least 500-fold for *conB*, 1,000-fold for *conC*, and 5,000-fold for *conD* (Fig. 2, rows c, e, and g). Attempts to improve complementation using alternative promoters to drive expression of the complemented gene were not successful (see Materials and Methods). The mating frequency of each strain was restored to near wild-type levels when a largely intact transfer-defective ICE*Bs1* was inserted elsewhere on the chromosome (data not shown), indicating that the in-frame deletions do not remove a *cis*-acting site required for conjugation. Partial complementation is observed commonly for conjugative systems (27, 46) and could be due to unexpected effects of the deletion on other ICE*Bs1* genes and/or insufficient expression of the complemented gene. Based on prior work (27), we suspect that the conjugation proteins are not efficiently translated and/or assembled into an active complex when expressed in *trans* to other ICE*Bs1* proteins. Nevertheless, we conclude that *conB*, *conC*, *conD*, and *conG* are critical for the conjugative transfer of ICE*Bs1*, while *yddF* appears to be dispensable under the conditions tested.

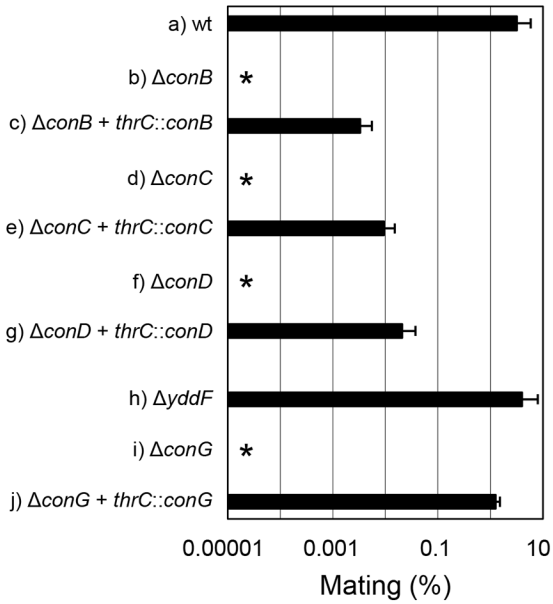

FIG 2 *conB*, *conC*, *conD*, and *conG* are required for mating of ICE*Bs1*. Cells were grown in minimal glucose medium. The indicated donor cells, all containing Δ(*rapI phrI*)*342*::*kan* in ICE*Bs1* and *amyE*::[Pspank(hy)-*rapI*], were mated with ICE*Bs1*^{0} *comK*::*cat str-84* recipient cells (CAL419). Percent mating is the number of transconjugant CFU per donor CFU times 100. Data are averages from at least three experiments. Error bars indicate the standard deviations. An asterisk indicates no detectable transconjugants (<1 × 10^{-5}%). Donor strains were JMA168 (a), MMB1275 (b), MMB1735 (c), MMB1271 (d), MMB1390 (e), MMB1274 (f), MMB1397 (g), MMB1273 (h), MMB1283 (i), and MMB1393 (j).

ICE*Bs1* genes required for the mobilization of plasmid pBS42. We predicted that *conB*, *conC*, *conD*, and *conG* are required for the conjugative transfer of ICE*Bs1* because they encode critical components of the ICE*Bs1* DNA translocation channel. Alternatively, these genes could be important for other aspects of ICE*Bs1* biology. For example, they could be critical for excision, replication, or integration of ICE*Bs1*. To distinguish these possibilities, we tested whether these genes were required for plasmid mobilization. Mobilization would require the ICE*Bs1* conjugation machinery but would not require genes involved in ICE*Bs1* DNA processing events (26).

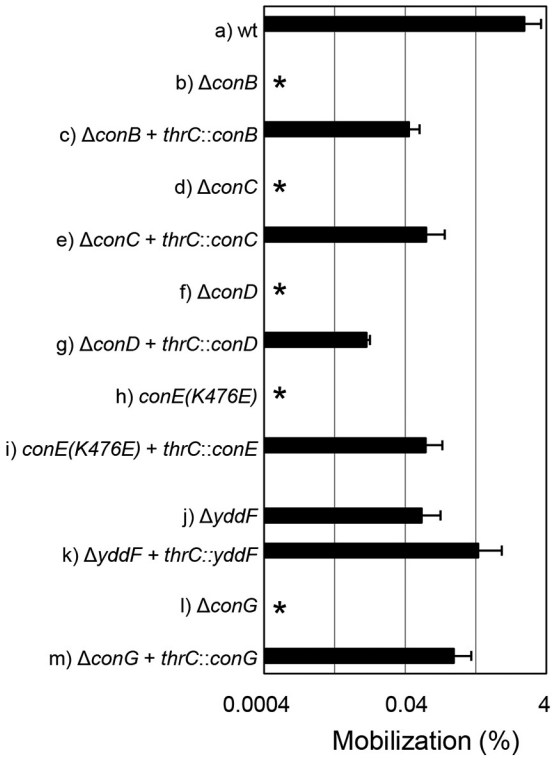

FIG 3 *conB*, *conC*, *conD*, *conE*, and *conG* are required for ICE*Bs1*-mediated mobilization of pBS42. Cells were grown in LB. The indicated donor cells, all containing pBS42 (*cam*) and Δ(*rapI phrI*)*342*::*kan* in ICE*Bs1* and *amyE*::[Pspank(hy)-*rapI*] were mated with ICE*Bs1*^{0} *comK*::*spc str-84* recipient cells (CAL89). Percent mobilization is the number of plasmid-bearing transconjugant CFU per donor CFU times 100. Data are averages from at least three experiments. Error bars indicate the standard deviations. An asterisk indicates no detectable plasmid-bearing transconjugants ($<4 \times 10^{-4}$%). Donor strains were MMB1473 (a), MMB1474 (b), MMB1760 (c), MMB1476 (d), MMB1477 (e), MMB1478 (f), MMB1479 (g), MMB1480 (h), MMB1481(i), MMB1482 (j), MMB1483 (k), MMB1484 (l), and MMB1485 (m).

We found that *conB*, *conC*, *conD*, *conE*, and *conG* were required for the ICE*Bs1*-mediated mobilization of plasmid pBS42 (Fig. 3). The same mating procedure as that described above was used, except that the ICE*Bs1*$^+$ donor strains also contained pBS42, a plasmid that confers chloramphenicol resistance, allowing the measurement of its acquisition. As seen previously (26), a wild-type donor strain (ICE*Bs1*$^+$) transferred pBS42 with an average mobilization frequency of ~2% (Fig. 3, row a). Mobilization of pBS42 was not detectable from donor strains containing deletions in *conB*, *conC*, *conD*, or *conG* or a donor strain containing a missense mutation (K476E) in the ATP-binding motif (Walker A box) of ConE (Fig. 3, rows b, d, f, h, and l). We estimate that plasmid mobilization is down at least 10,000-fold for each of these mutants. The Δ*yddF* donor strain mobilized pBS42 at a frequency of 0.07%, ~30-fold lower than that of the wild type (Fig. 3, row j), indicating that *yddF* contributes, at least modestly, to efficient pBS42 transfer. As observed for the mating assays, mobilization was partially complemented when the genes were expressed in *trans* (Fig. 3, rows c, e, g, i, k, and m). Taken together with their predicted membrane locations and sequence conservation, these results indicate that ConB, ConC, ConD, and ConG are components of the ICE*Bs1* DNA translocation channel, since they are required for both conjugation of ICE*Bs1* and plasmid mobilization. YddF does not seem to be a critical component of the channel, since it is not conserved in other conjugative elements, was not required for ICE*Bs1* transfer, and made only a minor contribution to plasmid mobilization.

***conB* and, to some extent, *conD* are required for ConE-GFP localization at the cell membrane.** ConE-GFP localizes to the membrane, predominantly at the cell poles, when ICE*Bs1* gene expression is induced (27). In contrast, ConE-GFP mislocalizes to the cytoplasm in cells lacking ICE*Bs1*. These results indicate that at least one ICE*Bs1* gene product recruits and/or retains ConE at the membrane. The four ICE*Bs1* proteins shown above to be required for both mating and mobilization (ConB, ConC, ConD, and ConG) all contain at least one predicted transmembrane helix (Fig. 1a). To test whether any of these proteins are required for ConE membrane localization, we examined the subcellular localization of ConE-GFP in strains containing large deletions of ICE*Bs1*. We used a construct in which *conE-gfp* is expressed from the ICE*Bs1* promoter Pxis, together with the upstream gene *conD*, at a heterologous locus (*lacA*) as previously described (27). *conD* was included upstream of *conE-gfp*, as ConE-GFP is not detectable in cells in the absence of *conD* in this context (data not shown). We observed ConE-GFP at the membrane, preferentially at the cell poles in cells containing an intact ICE*Bs1* (Fig. 4a), as seen previously (27). Furthermore, we found that ConE-GFP localized properly in a strain that contained a large deletion starting midway through *conG* and continuing through to *yddM* (Fig. 1b and 4b). Thus, ConE localization does not require the C terminus of ConG or the seven ICE*Bs1* proteins encoded downstream (CwlT, YddI, YddJ, YddK, RapI, PhrI, and YddM). In contrast, we found that ConE-GFP mislocalized to the cytoplasm in a strain containing a larger deletion spanning from *conB* to *yddM* (Fig. 1c and 4c). Previous experiments demonstrated that ConE-GFP expressed from *lacA* does not require wild-type *conE* in ICE*Bs1* for proper localization (27). Therefore, we conclude that ConB, ConC, ConD, YddF, and/or a part of ConG are required for localization of ConE-GFP.

To narrow down the requirements, we visualized ConE-GFP in strains containing single in-frame unmarked gene deletions. We found that ConE-GFP was dispersed throughout the cytoplasm in Δ*conB* cells (Fig. 4d). Localization was restored in Δ*conB* cells with addition of an ICE*Bs1* at an ectopic locus that contained the genes up to and including *conB* (Fig. 1d and data not shown), but localization was not restored with addition of an ICE*Bs1* that contained the genes up to but not including *conB* (Fig. 1e and data not shown), indicating that the defect in localization of ConE-GFP in the absence of *conB* was not due to the polarity of downstream genes. ConE-GFP targeted normally to the membrane in strains containing single-gene deletions of *conC*, *yddF*, or *conG* (Fig. 4e, g, and h). These results indicate that proper localization of ConE requires *conB* but not *conC* or any of the genes from *conE-yddM*.

Since expression of ConE-GFP at *lacA* required the presence of the upstream gene *conD*, we were unable to use this construct to test whether *conD* is required for ConE-GFP localization. Therefore, we fused *gfp* downstream of *conE* in its native position in ICE*Bs1*. To confirm that this new construct recapitulates ConE-GFP localization, we first examined ConE-GFP in this strain and in strains deleted for *conB* or *conC*. As expected, ConE-GFP localized properly in the parental and Δ*conC* strains but mislocalized in Δ*conB* cells (data not shown). We next examined ConE-GFP in

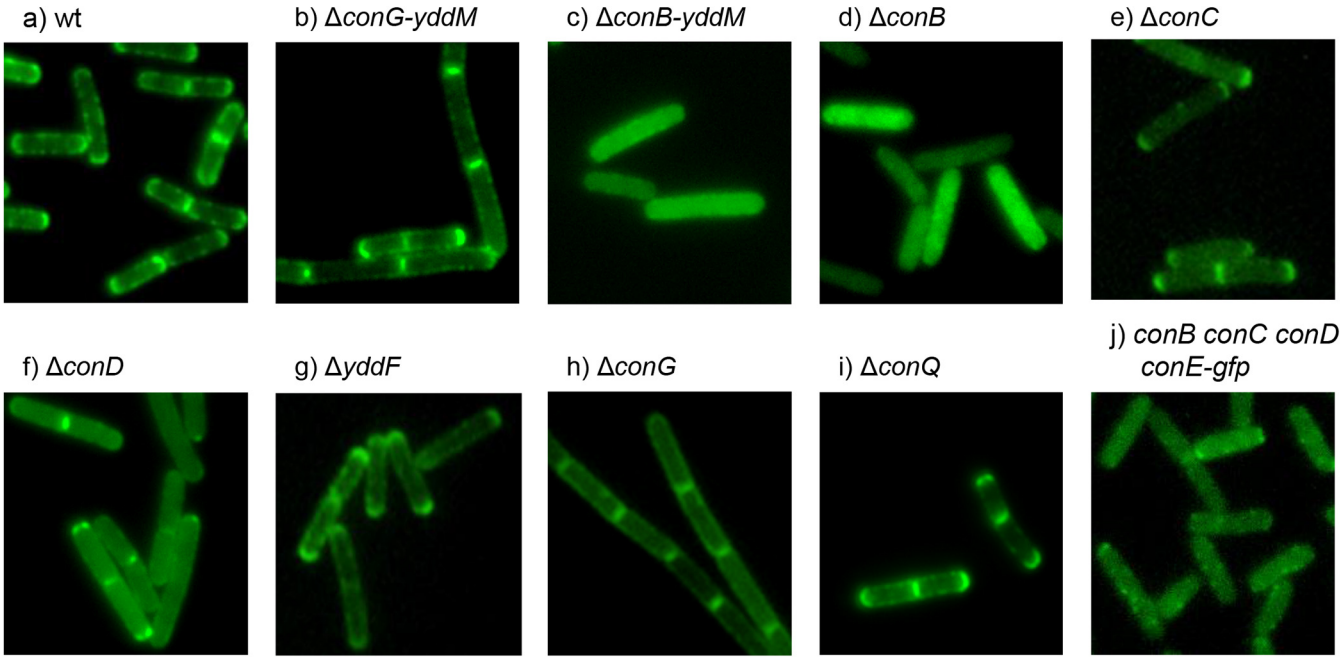

FIG 4 *conB* and, to some extent, *conD* are required for localization of ConE-GFP at the cell membrane. Cells were grown in minimal glucose medium. The indicated genotypes (Table 1) were analyzed by live fluorescence microscopy. ConE-GFP fluorescence is shown in green. Strains were MMB968 (a), MMB1425 (b), MMB1426 (c), MMB1297 (d), MMB1293 (e), MMB1549 (f), MMB1343 (g), MMB1299 (h), MMB1247 (i), and MMB1715 (j). All cells were induced with 1 mM IPTG for 1 h, except cells shown in panel h were induced for 2 h. ConE-GFP targeted normally in a strain deleted for *conG*, but the targeting required IPTG induction for 2 h instead of 1 h. We observed no differences in mating, mobilization, and ConE-GFP localization for 1 versus 2 h of induction for wild-type strains.

Δ*conD* cells. We observed a partial defect in localization in the Δ*conD* strain (Fig. 4f). ConE-GFP localized to the membrane preferentially at the cell poles in most cells; however, a large proportion of ConE-GFP also was found dispersed throughout the cytoplasm. Localization of ConE-GFP in a Δ*conD* strain was restored when *conD* was added back in *trans* (data not shown).

We also tested ConE-GFP localization in a Δ*conQ* strain, as ConQ is the only ICE*Bs1* transmembrane protein that had not been tested (Fig. 1a). We found that ConE-GFP localized normally in the absence of the presumed coupling protein ConQ (Fig. 4i). We conclude that ConB and, to some extent, ConD are required for recruiting and/or maintaining ConE at the membrane. Furthermore, our results show that *conQ*, *conC*, and the 10 genes from *conE* to *yddM* (Fig. 1a) are not required for ConE localization. Previously, we showed that *xis*, which encodes the excisionase, also was not required for ConE localization (27).

To determine whether ConB and ConD are sufficient for ConE's localization, we placed *conB*, *conC*, *conD*, and *conE-gfp* at an ectopic locus under the control of an inducible promoter. The genes were cloned in tandem, as arranged in ICE*Bs1*, and placed on the chromosome in a strain lacking ICE*Bs1*. We found that ConE-GFP largely mislocalized to the cytoplasm in these cells (Fig. 4j). Most cells contained several foci or clusters of GFP fluorescence, oftentimes localized near the membrane and cell poles. We hypothesize that the foci of ConE-GFP are formed due to the formation of subsets of the conjugation machinery proteins. When ConE-GFP is expressed in the presence of ConD alone, it mislocalizes to the cytoplasm uniformly and does not form small foci (27), indicating that ConB and/or ConC are involved in the formation of the clusters. Furthermore, the result indicates that while ConB and ConD are required for the localization of ConE to the membrane, they may not be sufficient. Ten ICE*Bs1* proteins encoded by genes upstream of *conB* (excluding ConQ and Xis) have not been tested and also may play a role. The best candidates include uncharacterized ICE*Bs1* proteins such as YdzL, YdcO, YdcS, YdcT, and YddA, although none of these are predicted membrane proteins. Alternatively, ConB and ConD may be sufficient, but they are not produced in the correct stoichiometry and/or targeted correctly when expressed from an ectopic locus. This second interpretation is consistent with our complementation data (Fig. 2 and 3) that indicate mating proteins do not function optimally when expressed *in trans*.

ConE and ConB interact in a bacterial two-hybrid assay. Our results indicate that ConB and, to some extent, ConD are required for localization of ConE to the membrane. To test whether ConE directly interacts with either protein, we used a bacterial two-hybrid assay that is based on the interaction between the T18 and T25 domains of the *Bordetella pertussis* enzyme adenylate cyclase (37). If the two domains are fused to interacting proteins, cyclic AMP is produced, resulting in increased expression of a *lacZ* reporter gene. Because the enzyme is cytoplasmic and does not rely on interactions with DNA, it has been useful for detecting interactions between membrane proteins, including components of T4SSs (40, 47–49). As we were uncertain as to whether the attachment of T18 or T25 at the N or C terminus of a protein would interfere with interaction or targeting, we made both types of fusions. Therefore, we constructed plasmids that encode ConE-T18 and T18-ConE, along with ConB-T25, T25-ConB, ConD-T25, and T25-ConD.

We cotransformed plasmids encoding T18 and T25 fusion

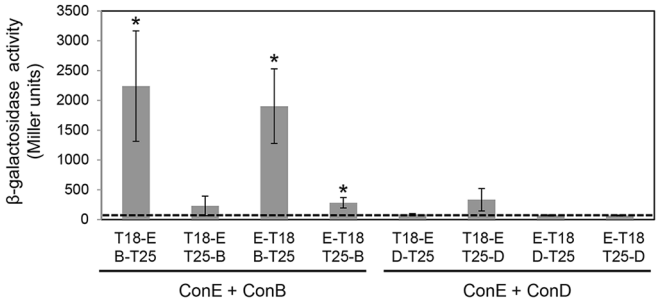

FIG 5 ConE interacts with ConB *in vivo* in bacterial two-hybrid assays. Quantitative β-galactosidase assays were performed on strains with plasmids expressing T18 and T25 fusion proteins. Strains contained plasmids expressing either T18-ConE (T18-E) or ConE-T18 (E-T18). Strains also contained a plasmid expressing ConB-T25 (B-T25), T25-ConB (T25-B), ConD-T25 (D-T25), or T25-ConD (T25-D). The average β-galactosidase activity and standard errors of the means are reported. The average β-galactosidase activity of the negative controls, expressing one fusion protein and one empty vector, is represented by the dotted line. A statistically significant *P* value (<0.05), as determined by a one-tailed heteroscedastic Student's *t* test comparing the experimental value versus the appropriate negative control, is indicated by an asterisk.

proteins and assayed their interactions by measuring β-galactosidase activity. Negative controls were cells cotransformed with one plasmid encoding a fusion protein (e.g., ConE-T18) and one empty vector. Of the four predator-prey ConE-ConB combinations tested, three showed statistically higher levels of β-galactosidase activity ($P < 0.05$) than the corresponding negative controls (~80 Miller units) (Fig. 5). No statistically significant interactions were detected between ConE and ConD (Fig. 5). These data indicate that ConE and ConB directly interact *in vivo*.

DISCUSSION

We found that *conB*, *conC*, *conD*, and *conG* are required for conjugative transfer of ICE*Bs1* and mobilization of pBS42. Homologs of these genes are found in other conjugative elements in Gram-positive bacteria and encode putative integral membrane proteins. We propose a model in which the ICE*Bs1* T4SS is composed of ConB, ConC, ConD, and ConG, along with the previously described ConE ATPase, presumed coupling protein ConQ, and cell wall hydrolase CwlT (Fig. 6). Similar models have been proposed recently for the conjugative plasmid pCW3 of *Clostridium perfringens* (10, 40, 46, 48, 50, 51), the broad-host-range conjugative plasmid pIP501 (12, 41, 52), and pCF10 of *Enterococcus faecalis* (11, 53, 54), indicating that a general consensus is building as to the composition of the Gram-positive T4SS.

ConG and ConB may form a major portion of the ICE*Bs1* DNA translocation channel within the membrane. ConG is large (815 amino acids long), and the N-terminal half is predicted to have seven transmembrane segments (Fig. 6). ConG likely forms higher-order oligomers, as seen for the Gram-positive homolog TcpH (47). ConB is shorter (354 amino acids long) and bitopic, with two tandem NTF2-like domains outside the cell membrane (40, 41). The extracytoplasmic domains of homologs of ConB crystallize as trimers. Given ConE's cytoplasmic location, we propose that ConE directly interacts with the short intracellular N-terminal tail of ConB (Fig. 6).

Recently, a low-resolution 3-MDa structure of a Gram-negative T4SS was determined using electron microscopy (55). Biochemical analysis of the complex indicates that most of the inner membrane components form very large oligomers within the T4SS. Notably, VirB3 and VirB8 appear to be 12-mers, VirB6 is a 24-mer, and VirB4 is associated with the T4SS as two separate hexameric rings on the cytoplasmic face of the complex. It will be interesting to determine whether the Gram-positive counterparts form a complex with similarly large oligomeric proportions.

In our model, the peripheral membrane protein ConE likely associates with the ICE*Bs1* T4SS through direct interaction with ConB. This interaction was supported by bacterial two-hybrid data (Fig. 5) and the observation that ConE-GFP's localization to the membrane depended upon *conB* (Fig. 4d). Two lines of evidence indicate a potential interaction between ConE and ConD. First, a large proportion of ConE-GFP mislocalizes to the cytoplasm in Δ*conD* cells (Fig. 4f). Second, *conD* and *conE* (and their homologs) are linked genetically. *conD* is encoded directly upstream of and translationally overlaps with *conE* in ICE*Bs1*. In

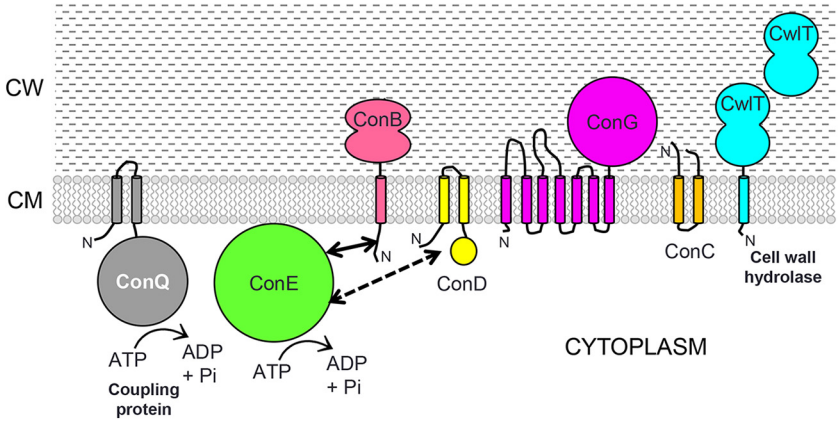

FIG 6 Model of localization and interactions of the ICE*Bs1* T4SS components. The cytoplasmic membrane (CM) and cell wall (CW) are indicated. N termini of proteins are indicated with an N. Topology predictions were obtained as described in the legend to Fig. 1 and have not been experimentally verified. The solid arrow indicates the interaction between ConE and ConB, consistent with ConE-GFP localization data and bacterial two-hybrid studies. A dotted arrow indicates the possible interaction between ConE and ConD, consistent with ConE-GFP localization data and their genetic linkage. No other interactions have been demonstrated. In the model, CwlT is drawn as a transmembrane protein and as a secreted protein, since it was observed to be both cell associated and in culture supernatants (9). The model does not depict oligomerization or interactions that have been demonstrated for other conjugative T4SSs.

many organisms, the *virB3*-like gene is directly fused to the *virB4* gene (8). Fusion of the T18 or T25 domain to ConE and ConD may have prevented their interaction in bacterial two-hybrid assays. More studies are necessary to address whether ConE and ConD indeed directly interact.

VirB4 proteins like ConE localize to the membrane, but the precise localization patterns are specific to each conjugative element. For example, TcpF of pCW3 localizes to the cell poles (47), and VirB4 of the *B. subtilis* plasmid pLS20 localizes at a single pole and at several sites along the membrane (56). In contrast, both VirB4 of *A. tumefaciens* and TrhC of the *E. coli* R27 conjugative plasmid localize to several foci along the periphery of the cell membrane (57, 58). While ConE requires only two of the seven other known ICE*Bs1* T4SS proteins for its localization, TrhC requires 12 different R27 T4SS proteins (58). All 12 proteins likely do not interact directly with TrhC; rather, this group of proteins may form an ordered network of interacting proteins whereby disruption of initializing components could result in incomplete assembly and mislocalization of TrhC.

The ICE*Bs1* protein YddF was not required for conjugation and is not conserved in other conjugative elements. While the function of YddF still is unclear, our results indicate that this putative DNA-binding protein in part facilitates plasmid mobilization (Fig. 3). This effect could be indirect, such as *yddF* increasing pBS42 copy number. While YddF was dispensable for transfer of ICE*Bs1* under our conditions, YddF could be required when mating into other types of bacteria or under different conditions. Nevertheless, YddF is not a critical component of the ICE*Bs1* T4SS.

Together, our results provide a first model for the T4SS of ICE*Bs1* (Fig. 6). Future experiments will be required to verify the predicted topologies of the protein components and determine their protein-protein interactions and functions.

ACKNOWLEDGMENTS

We thank Suffolk undergraduate students Naira Aleksanyan, Georgeanna Morton, April Culannay, Stefanie Baril, Omar Pinkhasov, and former class members of CHEM L333 for their contributions to this project. We thank Edith Enyedy for technical assistance and the chemistry and biology faculty at Suffolk University for their support. We thank Jacob Thomas at the Georgia Institute of Technology and Briana Burton of Harvard University for helpful advice, Kenneth Briley and David Dubnau at the Public Health Research Institute for useful vectors, and Laurel Wright and Chris Johnson of the Massachusetts Institute of Technology for helpful comments on the manuscript.

This work was supported in part by the National Science Foundation Research at Undergraduate Institution program (NSF-RUI grant 1157878 to M.B.B.), the National Institute of General Medical Sciences of the National Institutes of Health (R01GM50895 to A.D.G.), and a Suffolk University Summer Stipend Award (M.B.B.).

REFERENCES

1. **Wiedenbeck J, Cohan FM.** 2011. Origins of bacterial diversity through horizontal genetic transfer and adaptation to new ecological niches. FEMS Microbiol Rev **35:**957–976. http://dx.doi.org/10.1111/j.1574-6976.2011.00292.x.
2. **Gogarten JP, Townsend JP.** 2005. Horizontal gene transfer, genome innovation and evolution. Nat Rev Microbiol **3:**679–687. http://dx.doi.org/10.1038/nrmicro1204.
3. **Frost LS, Leplae R, Summers AO, Toussaint A.** 2005. Mobile genetic elements: the agents of open source evolution. Nat Rev Microbiol **3:**722–732. http://dx.doi.org/10.1038/nrmicro1235.
4. **Waksman G, Fronzes R.** 2010. Molecular architecture of bacterial type IV secretion systems. Trends Biochem Sci **35:**691–698. http://dx.doi.org/10.1016/j.tibs.2010.06.002.
5. **Smillie C, Garcillan-Barcia MP, Francia MV, Rocha EP, de la Cruz F.** 2010. Mobility of plasmids. Microbiol Mol Biol Rev **74:**434–452. http://dx.doi.org/10.1128/MMBR.00020-10.
6. **Goessweiner-Mohr N, Arends K, Keller W, Grohmann E.** 2013. Conjugative type IV secretion systems in Gram-positive bacteria. Plasmid **70:**289–302. http://dx.doi.org/10.1016/j.plasmid.2013.09.005.
7. **Bhatty M, Laverde Gomez JA, Christie PJ.** 2013. The expanding bacterial type IV secretion lexicon. Res Microbiol **164:**620–639. http://dx.doi.org/10.1016/j.resmic.2013.03.012.
8. **Alvarez-Martinez CE, Christie PJ.** 2009. Biological diversity of prokaryotic type IV secretion systems. Microbiol Mol Biol Rev **73:**775–808. http://dx.doi.org/10.1128/MMBR.00023-09.
9. **DeWitt T, Grossman AD.** 2014. The bifunctional cell wall hydrolase CwlT is needed for conjugation of the integrative and conjugative element ICE*Bs1* in *Bacillus subtilis* and *B. anthracis*. J Bacteriol **196:**1588–1596. http://dx.doi.org/10.1128/JB.00012-14.
10. **Bantwal R, Bannam TL, Porter CJ, Quinsey NS, Lyras D, Adams V, Rood JI.** 2012. The peptidoglycan hydrolase TcpG is required for efficient conjugative transfer of pCW3 in *Clostridium perfringens*. Plasmid **67:**139–147. http://dx.doi.org/10.1016/j.plasmid.2011.12.016.
11. **Laverde Gomez JA, Bhatty M, Christie PJ.** 2014. PrgK, a multidomain peptidoglycan hydrolase, is essential for conjugative transfer of the pheromone-responsive plasmid pCF10. J Bacteriol **196:**527–539. http://dx.doi.org/10.1128/JB.00950-13.
12. **Arends K, Celik EK, Probst I, Goessweiner-Mohr N, Fercher C, Grumet L, Soellue C, Abajy MY, Sakinc T, Broszat M, Schiwon K, Koraimann G, Keller W, Grohmann E.** 2013. TraG encoded by the pIP501 type IV secretion system is a two-domain peptidoglycan-degrading enzyme essential for conjugative transfer. J Bacteriol **195:**4436–4444. http://dx.doi.org/10.1128/JB.02263-12.
13. **Berger BR, Christie PJ.** 1994. Genetic complementation analysis of the *Agrobacterium tumefaciens virB* operon: *virB2* through *virB11* are essential virulence genes. J Bacteriol **176:**3646–3660.
14. **Bayer M, Eferl R, Zellnig G, Teferle K, Dijkstra A, Koraimann G, Hogenauer G.** 1995. Gene 19 of plasmid R1 is required for both efficient conjugative DNA transfer and bacteriophage R17 infection. J Bacteriol **177:**4279–4288.
15. **Winans SC, Walker GC.** 1985. Conjugal transfer system of the IncN plasmid pKM101. J Bacteriol **161:**402–410.
16. **Berkmen MB, Laurer SJ, Giarusso BK, Romero R.** 2013. The integrative and conjugative element ICE*Bs1* of *Bacillus subtilis*. *In* Roberts AP, Mullany P (ed), Bacterial integrative mobile genetic elements. Landes Biosciences, Austin, TX.
17. **Babic A, Berkmen MB, Lee CA, Grossman AD.** 2011. Efficient gene transfer in bacterial cell chains. mBio **2**(2):e00027–11. http://dx.doi.org/10.1128/mBio.00027-11.
18. **Thomas J, Lee CA, Grossman AD.** 2013. A conserved helicase processivity factor is needed for conjugation and replication of an integrative and conjugative element. PLoS Genet **9:**e1003198. http://dx.doi.org/10.1371/journal.pgen.1003198.
19. **Auchtung JM, Lee CA, Garrison KL, Grossman AD.** 2007. Identification and characterization of the immunity repressor (ImmR) that controls the mobile genetic element ICE*Bs1* of *Bacillus subtilis*. Mol Microbiol **64:**1515–1528. http://dx.doi.org/10.1111/j.1365-2958.2007.05748.x.
20. **Auchtung JM, Lee CA, Monson RE, Lehman AP, Grossman AD.** 2005. Regulation of a *Bacillus subtilis* mobile genetic element by intercellular signaling and the global DNA damage response. Proc Natl Acad Sci U S A **102:**12554–12559. http://dx.doi.org/10.1073/pnas.0505835102.
21. **Bose B, Auchtung JM, Lee CA, Grossman AD.** 2008. A conserved anti-repressor controls horizontal gene transfer by proteolysis. Mol Microbiol **70:**570–582. http://dx.doi.org/10.1111/j.1365-2958.2008.06414.x.
22. **Bose B, Grossman AD.** 2011. Regulation of horizontal gene transfer in *Bacillus subtilis* by activation of a conserved site-specific protease. J Bacteriol **193:**22–29. http://dx.doi.org/10.1128/JB.01143-10.
23. **Lee CA, Auchtung JM, Monson RE, Grossman AD.** 2007. Identification and characterization of *int* (integrase), *xis* (excisionase) and chromosomal attachment sites of the integrative and conjugative element ICE*Bs1* of *Bacillus subtilis*. Mol Microbiol **66:**1356–1369. http://dx.doi.org/10.1111/j.1365-2958.2007.06000.x.
24. **Lee CA, Babic A, Grossman AD.** 2010. Autonomous plasmid-like replication of a conjugative transposon. Mol Microbiol **75:**268–279. http://dx.doi.org/10.1111/j.1365-2958.2009.06985.x.
25. **Lee CA, Grossman AD.** 2007. Identification of the origin of transfer

(*oriT*) and DNA relaxase required for conjugation of the integrative and conjugative element ICE*Bs1* of *Bacillus subtilis*. J Bacteriol **189:**7254–7261. http://dx.doi.org/10.1128/JB.00932-07.
26. **Lee CA, Thomas J, Grossman AD.** 2012. The *Bacillus subtilis* conjugative transposon ICE*Bs1* mobilizes plasmids lacking dedicated mobilization functions. J Bacteriol **194:**3165–3172. http://dx.doi.org/10.1128/JB.00301-12.
27. **Berkmen MB, Lee CA, Loveday EK, Grossman AD.** 2010. Polar positioning of a conjugation protein from the integrative and conjugative element ICE*Bs1* of *Bacillus subtilis*. J Bacteriol **192:**38–45. http://dx.doi.org/10.1128/JB.00860-09.
28. **Johnson CM, Grossman AD.** 2014. Identification of host genes that affect acquisition of an integrative and conjugative element in *Bacillus subtilis*. Mol Microbiol **93:**1284–1301. http://dx.doi.org/10.1111/mmi.12736.
29. **Vasantha N, Freese E.** 1980. Enzyme changes during *Bacillus subtilis* sporulation caused by deprivation of guanine nucleotides. J Bacteriol **144:**1119–1125.
30. **Harwood CR, Cutting SM.** 1990. Molecular Biological Methods for *Bacillus*. John Wiley & Sons, Chichester, United Kingdom.
31. **Perego M, Spiegelman GB, Hoch JA.** 1988. Structure of the gene for the transition state regulator, *abrB*: regulator synthesis is controlled by the *spo0A* sporulation gene in *Bacillus subtilis*. Mol Microbiol **2:**689–699. http://dx.doi.org/10.1111/j.1365-2958.1988.tb00079.x.
32. **Horton RM, Hunt HD, Ho SN, Pullen JK, Pease LR.** 1989. Engineering hybrid genes without the use of restriction enzymes: gene splicing by overlap extension. Gene **77:**61–68. http://dx.doi.org/10.1016/0378-1119(89)90359-4.
33. **Comella N, Grossman AD.** 2005. Conservation of genes and processes controlled by the quorum response in bacteria: characterization of genes controlled by the quorum-sensing transcription factor ComA in *Bacillus subtilis*. Mol Microbiol **57:**1159–1174. http://dx.doi.org/10.1111/j.1365-2958.2005.04749.x.
34. **Gibson DG, Young L, Chuang RY, Venter JC, Hutchison CA, III, Smith HO.** 2009. Enzymatic assembly of DNA molecules up to several hundred kilobases. Nat Methods **6:**343–345. http://dx.doi.org/10.1038/nmeth.1318.
35. **Simmons LA, Davies BW, Grossman AD, Walker GC.** 2008. Beta clamp directs localization of mismatch repair in *Bacillus subtilis*. Mol Cell **29:**291–301. http://dx.doi.org/10.1016/j.molcel.2007.10.036.
36. **Lemon KP, Grossman AD.** 1998. Localization of bacterial DNA polymerase: evidence for a factory model of replication. Science **282:**1516–1519. http://dx.doi.org/10.1126/science.282.5393.1516.
37. **Karimova G, Ullmann A, Ladant D.** 2000. A bacterial two-hybrid system that exploits a cAMP signaling cascade in *Escherichia coli*. Methods Enzymol **328:**59–73. http://dx.doi.org/10.1016/S0076-6879(00)28390-0.
38. **Miller JH.** 1972. Experiments in Molecular Genetics. Cold Spring Harbor Laboratory Press, Cold Spring Harbor, NY.
39. **Berkmen MB, Grossman AD.** 2006. Spatial and temporal organization of the *Bacillus subtilis* replication cycle. Mol Microbiol **62:**57–71. http://dx.doi.org/10.1111/j.1365-2958.2006.05356.x.
40. **Porter CJ, Bantwal R, Bannam TL, Rosado CJ, Pearce MC, Adams V, Lyras D, Whisstock JC, Rood JI.** 2012. The conjugation protein TcpC from *Clostridium perfringens* is structurally related to the type IV secretion system protein VirB8 from Gram-negative bacteria. Mol Microbiol **83:**275–288. http://dx.doi.org/10.1111/j.1365-2958.2011.07930.x.
41. **Goessweiner-Mohr N, Grumet L, Arends K, Pavkov-Keller T, Gruber CC, Gruber K, Birner-Gruenberger R, Kropec-Huebner A, Huebner J, Grohmann E, Keller W.** 2013. The 2.5 Å structure of the *Enterococcus* conjugation protein TraM resembles VirB8 type IV secretion proteins. J Biol Chem **288:**2018–2028. http://dx.doi.org/10.1074/jbc.M112.428847.
42. **Keller J, Leulliot N, Cambillau C, Campanacci V, Porciero S, Prangishvilli D, Forterre P, Cortez D, Quevillon-Cheruel S, van Tilbeurgh H.** 2007. Crystal structure of AFV3-109, a highly conserved protein from crenarchaeal viruses. Virol J **4:**12. http://dx.doi.org/10.1186/1743-422X-4-12.
43. **Larson ET, Eilers BJ, Reiter D, Ortmann AC, Young MJ, Lawrence CM.** 2007. A new DNA binding protein highly conserved in diverse crenarchaeal viruses. Virology **363:**387–396. http://dx.doi.org/10.1016/j.virol.2007.01.027.
44. **Wozniak RA, Waldor MK.** 2010. Integrative and conjugative elements: mosaic mobile genetic elements enabling dynamic lateral gene flow. Nat Rev Microbiol **8:**552–563. http://dx.doi.org/10.1038/nrmicro2382.
45. **Burrus V, Waldor MK.** 2004. Shaping bacterial genomes with integrative and conjugative elements. Res Microbiol **155:**376–386. http://dx.doi.org/10.1016/j.resmic.2004.01.012.
46. **Bannam TL, Teng WL, Bulach D, Lyras D, Rood JI.** 2006. Functional identification of conjugation and replication regions of the tetracycline resistance plasmid pCW3 from *Clostridium perfringens*. J Bacteriol **188:**4942–4951. http://dx.doi.org/10.1128/JB.00298-06.
47. **Teng WL, Bannam TL, Parsons JA, Rood JI.** 2008. Functional characterization and localization of the TcpH conjugation protein from *Clostridium perfringens*. J Bacteriol **190:**5075–5086. http://dx.doi.org/10.1128/JB.00386-08.
48. **Steen JA, Bannam TL, Teng WL, Devenish RJ, Rood JI.** 2009. The putative coupling protein TcpA interacts with other pCW3-encoded proteins to form an essential part of the conjugation complex. J Bacteriol **191:**2926–2933. http://dx.doi.org/10.1128/JB.00032-09.
49. **de Paz HD, Larrea D, Zunzunegui S, Dehio C, de la Cruz F, Llosa M.** 2010. Functional dissection of the conjugative coupling protein TrwB. J Bacteriol **192:**2655–2669. http://dx.doi.org/10.1128/JB.01692-09.
50. **Wisniewski JA, Teng WL, Bannam TL, Rood JI.** 2015. Two novel membrane proteins TcpD and TcpE are essential for conjugative transfer of pCW3 in *Clostridium perfringens*. J Bacteriol **197:**774–781. http://dx.doi.org/10.1128/JB.02466-14.
51. **Parsons JA, Bannam TL, Devenish RJ, Rood JI.** 2007. TcpA, an FtsK/SpoIIIE homolog, is essential for transfer of the conjugative plasmid pCW3 in *Clostridium perfringens*. J Bacteriol **189:**7782–7790. http://dx.doi.org/10.1128/JB.00783-07.
52. **Abajy MY, Kopec J, Schiwon K, Burzynski M, Doring M, Bohn C, Grohmann E.** 2007. A type IV-secretion-like system is required for conjugative DNA transport of broad-host-range plasmid pIP501 in gram-positive bacteria. J Bacteriol **189:**2487–2496. http://dx.doi.org/10.1128/JB.01491-06.
53. **Li F, Alvarez-Martinez C, Chen Y, Choi KJ, Yeo HJ, Christie PJ.** 2012. *Enterococcus faecalis* PrgJ, a VirB4-like ATPase, mediates pCF10 conjugative transfer through substrate binding. J Bacteriol **194:**4041–4051. http://dx.doi.org/10.1128/JB.00648-12.
54. **Chen Y, Zhang X, Manias D, Yeo HJ, Dunny GM, Christie PJ.** 2008. *Enterococcus faecalis* PcfC, a spatially localized substrate receptor for type IV secretion of the pCF10 transfer intermediate. J Bacteriol **190:**3632–3645. http://dx.doi.org/10.1128/JB.01999-07.
55. **Low HH, Gubellini F, Rivera-Calzada A, Braun N, Connery S, Dujeancourt A, Lu F, Redzej A, Fronzes R, Orlova EV, Waksman G.** 2014. Structure of a type IV secretion system. Nature **508:**550–553. http://dx.doi.org/10.1038/nature13081.
56. **Bauer T, Rosch T, Itaya M, Graumann PL.** 2011. Localization pattern of conjugation machinery in a Gram-positive bacterium. J Bacteriol **193:**6244–6256. http://dx.doi.org/10.1128/JB.00175-11.
57. **Aguilar J, Cameron TA, Zupan J, Zambryski P.** 2011. Membrane and core periplasmic *Agrobacterium tumefaciens* virulence Type IV secretion system components localize to multiple sites around the bacterial perimeter during lateral attachment to plant cells. mBio **2**(6):e00218–00211. http://dx.doi.org/10.1128/mBio.00218-11.
58. **Gilmour MW, Taylor DE.** 2004. A subassembly of R27-encoded transfer proteins is dependent on TrhC nucleoside triphosphate-binding motifs for function but not formation. J Bacteriol **186:**1606–1613. http://dx.doi.org/10.1128/JB.186.6.1606-1613.2004.
59. **Käll L, Krogh A, Sonnhammer EL.** 2005. An HMM posterior decoder for sequence feature prediction that includes homology information. Bioinformatics **21**(Suppl 1)**:**i251–i257. http://dx.doi.org/10.1093/bioinformatics/bti1014.
60. **Zhou M, Boekhorst J, Francke C, Siezen RJ.** 2008. LocateP: genome-scale subcellular-location predictor for bacterial proteins. BMC Bioinformatics **9:**173. http://dx.doi.org/10.1186/1471-2105-9-173.